

Disordering and dissolution of γ' precipitates under ion irradiation

Françoise Bourdeau, Eric Camus, Christian Abromeit, and Heinrich Wollenberger

Hahn-Meitner-Institut Berlin GmbH, Glienicker Straße 100, D-14109 Berlin, Federal Republic of Germany

(Received 27 June 1994)

The stability of the γ' phase of the nickel-base alloy Nimonic PE16 under irradiation with Ni^+ ions of 300-keV energy is studied by means of transmission electron microscopy. The disordering of the γ' phase could be followed as a function of fluence. The main finding is the observation of weak but measurable superlattice reflections between 0.1 and 1 dpa after irradiation at room temperature. The superlattice reflections disappear in two steps. Their intensities decrease considerably within a fluence of 0.1 dpa, while weak intensities are observed up to a fluence of 1 dpa. These reflections disappear completely after a fluence of 2 dpa. The results are discussed within a model which considers both disordering and dissolution of precipitates under cascade producing irradiation.

I. INTRODUCTION

Irradiation with energetic particles influence the microstructure of materials significantly. Processes such as precipitation of new phases, dissolution of equilibrium phases and the production of defect structures limit the stability of a material in a radiation environment and are therefore investigated in many different systems. In the case of ordered precipitates, mainly two processes determine the stability of the precipitates under irradiation: (i) the disordering of the ordered phase and (ii) the dissolution of the precipitates by atomic mixing. The investigation of both processes is therefore necessary for an understanding of radiation effects in such materials and for a prediction of the microstructural evolution under irradiation.

The stability of ordered precipitates under ion irradiation was studied earlier^{1,2} for the γ/γ' technical alloy Nimonic PE16 by means of transmission electron microscopy (TEM). The decrease in intensity of the superlattice reflections, which indicates a decreasing degree of order in the specimen, was taken to estimate the dissolution rate of the γ' phase. The authors proposed a disorder-dissolution model for the dissolution of ordered precipitates based upon certain assumptions about the coupling of the disordering and dissolution processes. However, as no direct measurement of the changes in the concentration profile around the precipitates existed, the disordering process could not be distinguished from the dissolution one.

Recently, Martin and co-workers³⁻⁶ have proposed a more detailed theoretical description of the evolution of ordered precipitates under irradiation, which allows to calculate simultaneously the degree of order and the concentration profile around a precipitate as a function of irradiation parameters in the case of ordered B_2 and $L1_2$ structures.^{5,6} They predict significant differences between the respective stability in the degree of order inside the precipitate and the concentration profile around the precipitate, respectively.

This paper deals with the experimental investigation of the disordering and dissolution mechanisms of precipi-

tates under ion irradiation. $L1_2$ -ordered γ' precipitates are irradiated with Ni^+ ions of 300-keV energy at room temperature. The evolution of the order in the γ' phase as a function of irradiation time was followed by observing the changes in the intensities of superlattice reflections by means of TEM. As the dissolution of the precipitates could be studied by field-ion microscopy with atom probe (FIM-AP) independently of the state of order of the γ' phase, the disordering and the dissolution processes could be investigated separately.

In Sec. II we report on the specimen preparation and on the experimental technique for imaging of the γ' phase with TEM. The results of the irradiation experiments are given in Sec. III. The discussion of the experimental results and the comparison with model calculations are presented in Sec. IV.

II. EXPERIMENTAL TECHNIQUES

A. Specimen preparation

The technical alloy Nimonic PE16 is a nickel-base alloy containing mainly Fe (34 at. %), Cr (16 at. %), Al (2.7 at. %), Ti (1.5 at. %) and Mo (2 at. %). An appropriate thermal aging following solution treatment leads to the precipitation of spherical γ' precipitates, the volume fraction of which lies between 3 and 10%. Both the γ' phase and matrix γ phase have a face-centered-cubic structure with lattice constants of 0.359 15 and 0.359 25 nm at room temperature, respectively. The γ' precipitates are coherent with the γ matrix. The lattice distance misfit amounts to about 0.03%.

The small quantities of C and N (less than 0.2 and 0.02 at. %, respectively) present in the alloy lead to the precipitation of carbides and nitrides. Their volume fraction is less than 1%.

The kinetics of precipitation of carbides and γ' phase under thermal treatment has been investigated in detail in previous works by means of various complementary experimental techniques: field-ion microscopy with atom probe, small-angle neutron scattering and transmission electron microscopy with energy-dispersive analysis.⁷

The evolution of particle size and particle number density has been investigated in a broad range of aging temperatures and times. Therefore, the precipitate size and number density appropriate for the present investigation techniques could be adjusted accordingly.

The alloy Nimonic PE16 was delivered by Glossop Superalloys Limited. The specimens were solution annealed at 1313 K for 2 h under argon atmosphere and quenched in water. A precipitate diameter of 19 ± 4 nm was prepared by subsequent aging at 1025 K for 24 h under argon atmosphere. The obtained volume fraction was 0.06 ± 0.02 . These data are in good agreement with those of Degischer *et al.*⁷ obtained under similar thermal treatment.

The TEM specimens to be irradiated were electrolytically thinned to a thickness of $10 \mu\text{m}$ in a solution of dilute perchloric acid. After irradiation, they were back polished from the unirradiated surface until perforation occurred.

B. Detection of the γ' phase by TEM

The γ' phase is ordered with a $L1_2$ structure (Cu_3Au type). Hence the γ' precipitates can be easily imaged in dark-field mode with a superlattice reflection. Figure 1 shows a dark-field image of the γ' phase imaged with a $\{210\}$ superlattice reflection. We have also used a bright-field technique to image the precipitates. The nonirradiated γ' precipitates can be imaged using a conventional bright-field imaging technique.⁷ We however found *thickness contrast* imaging⁸ of the precipitates to be more sensitive. If the thickness of the foil increases as the distance from the foil edge increases, then thickness fringes, which correspond to successive minima and maxima in the intensity, will appear. As the γ' phase is richer in Al content as compared to the γ phase, its extinction distance is larger than that of the matrix. The pres-

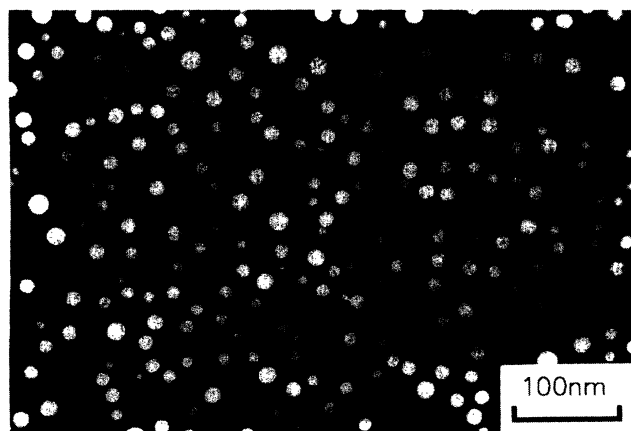


FIG. 1. Dark-field image of the γ' phase after solution annealing at 1313 K for 2 h and subsequent aging at 1025 K for 24 h. A $\{210\}$ superlattice reflection in the $\langle 211 \rangle$ reciprocal plane was used for imaging. The mean diameter of the precipitates and the volume fraction of the γ' phase are 19 ± 4 nm and 0.06 ± 0.02 , respectively.

ence of a γ' precipitate in the changing thickness region of the foil therefore results in a change locally of the effective thickness of the foil. As a consequence, the γ' precipitates will be imaged alternately in dark and bright contrast differently from the matrix.⁸ The contrast will be stronger at places where the intensity varies rapidly with the foil thickness. The contrast observed experimentally is shown in Fig. 2.

The knowledge of the foil thickness is, on the one hand, necessary for the determination of the volume fraction of the precipitates, and, on the other hand, it is of great importance for investigating the irradiation effects, because of the limited range of the ion damage. The foil thickness can be determined from convergent beam diffraction patterns.⁹ However, this procedure could not be used in the case of irradiated specimens because of the high density of radiation-induced defects (dislocation loops, small voids, etc.) in the specimens. Therefore, we used the method proposed by Reed,¹⁰ which is based on the property that the intensity of the x-rays produced in the specimen by the electron beam bombardment is a function of the foil thickness. Using the energy dispersive x-ray analysis attachment to the TEM, the intensity of the x-rays for different foil thicknesses was calibrated for a nonirradiated specimen. The corresponding foil thickness was measured using the convergent beam technique. The foil thicknesses in the irradiated specimens were then determined by measuring the x-ray intensity and using the calibration curve of x-ray intensity vs foil thickness.¹¹

An important feature of the Nimonic PE16 alloy is the small volume fraction of the γ' phase, which is due to the low Al and Ti content in the alloy. This feature is obviously favorable for a theoretical treatment, as the precipitates can be treated as being isolated in the matrix. On the other hand, this fact precludes any quantitative determination of the degree of order of the precipitates, as the intensity of the superlattice reflections is correspondingly small. In the present investigation, we will report on the



FIG. 2. Bright-field image of the γ' phase with a thickness contrast. The γ' precipitates have a larger extinction distance than the matrix and are imaged alternately in bright and dark contrast.

qualitative evolution of the intensity of the superlattice reflections in the $\langle 211 \rangle$ reciprocal plane as a function of fluence.

III. IRRADIATION EXPERIMENTS

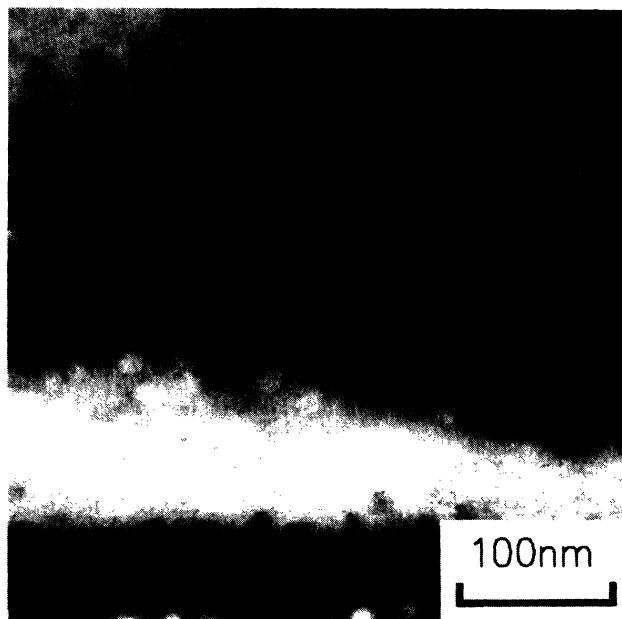
The irradiation experiments were performed by using $^{58}\text{Ni}^+$ ions of 300 keV. The specimens were irradiated across an area of 2 mm diameter with a beam current density of $\Phi = 5 \times 10^{15} \text{ m}^{-2} \text{ s}^{-1}$. The total cross section σ_d for recoils above the displacement energy of 40 eV was evaluated with the use of the simulation program TRIM.¹² The damage between the surface and a depth of 100 nm varies only slightly. The mean total cross section amounts to $\sigma_d = 2 \times 10^{-19} \text{ m}^2$.¹³ The resulting displacement rate K in displacements per atom and per second (dpa s^{-1}), is given by $K = \sigma_d \Phi$ and amounts to $10^{-3} \text{ dpa s}^{-1}$ in the present investigation.

All irradiation experiments included in this paper were performed at room temperature. The fluence varied between 0.001 and 2 dpa. Figure 3 shows a dark-field image of the γ' phase after irradiation with a fluence of 0.05 dpa. Small dark areas can be seen within the precipitates showing local influence of the displacement cascades. Dark-field imaging of the γ' precipitates at higher fluences was not possible due to the very low intensity of the superlattice reflections. The precipitates could, however, be imaged even after irradiation with fluences of 1 and 2 dpa using the thickness contrast imaging technique as described in the previous section. Examples of such images are shown in Figs. 4(a) and 4(b). A qualitative comparison shows that the size of the precipitates is unchanged when compared to the nonirradiated state.

The disordering kinetics of the γ' phase was followed by comparing the intensity of the superlattice reflections in $\langle 211 \rangle$ zone axis diffraction patterns in specimens irradiated to different degree. The observed decrease of the

intensity of the superlattice reflections after irradiation with increasing fluences is illustrated in Fig. 5. Figure 5(a) shows a diffraction pattern from $\langle 211 \rangle$ zone axis from specimen in the aged state before irradiation (see Fig. 1). The superlattice reflection is clearly visible and its intensity is fairly strong. Figure 5(b) demonstrates the decrease in the intensity of the superlattice reflections after irradiation with a fluence of 0.1 dpa. Between 0.1 and 1 dpa, only a very weak residual intensity can be observed [Fig. 5(c)]. However, as the intensity of the super-

(a)



(b)

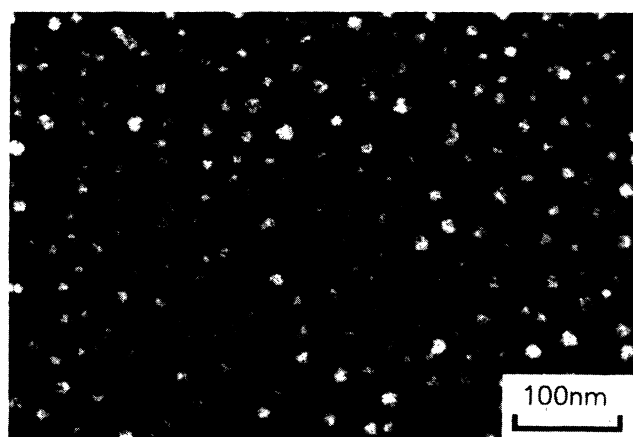
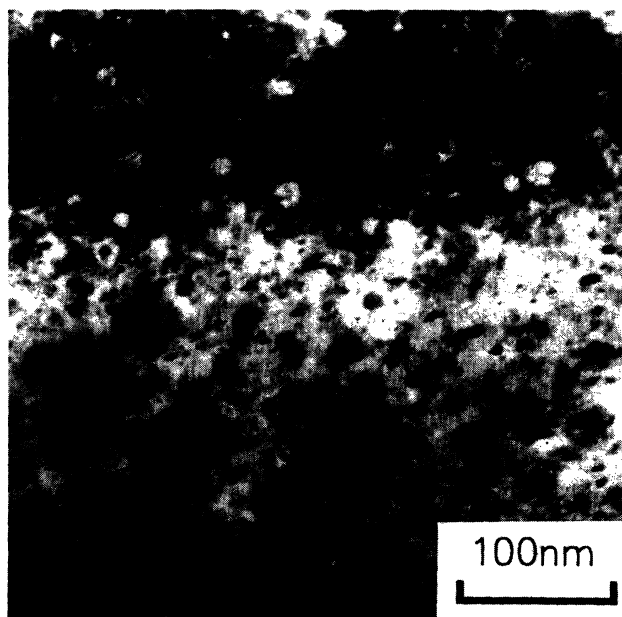


FIG. 3. Dark-field image of the γ' precipitates after irradiation with Ni self-ions at room temperature with a displacement rate of $10^{-3} \text{ dpa s}^{-1}$ to a fluence of 0.05 dpa. A $\{210\}$ superlattice reflection in the $\langle 211 \rangle$ reciprocal plane was used for imaging.

FIG. 4. Bright-field image of the γ' precipitates after irradiation with Ni self-ions at room temperature with a displacement rate of $10^{-3} \text{ dpa s}^{-1}$ to fluences of (a) 1 dpa and (b) 2 dpa.

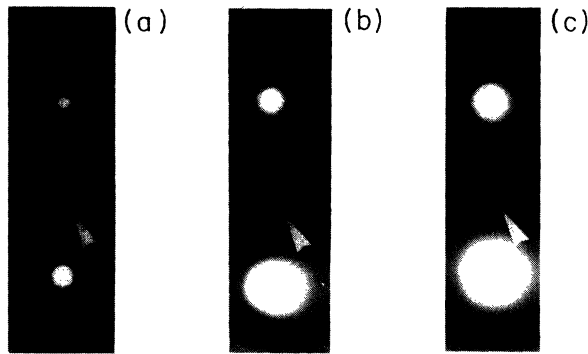


FIG. 5. Diffraction patterns of γ' containing specimens (a) before irradiation and after irradiation with Ni self-ions at room temperature with a displacement rate of 10^{-3} dpa s^{-1} to fluences of (b) 0.1 dpa and (c) 1 dpa.

lattice reflections is very weak, a quantitative evaluation was not possible. The intensity vanishes after an irradiation of 2 dpa. The same qualitative behavior of a two-step process was observed for the displacement rates of 10^{-4} dpa s^{-1} and 10^{-2} dpa s^{-1} , i.e., a first rapid reduction of the intensity of the superlattice reflections within 0.1 dpa and its disappearance with fluences larger than 1 dpa.

From the qualitative analysis of dark-field images, bright-field images and of diffraction patterns, we can conclude that at room temperature (i) the γ' phase disorders for the most part already after a fluence of 0.1 dpa; (ii) a residual intensity of superlattice reflections is observed up to fluences of 1 dpa; (iii) after a fluence of 2 dpa, the superlattice reflections disappear while the precipitates can yet be imaged in bright field.

IV. DISCUSSION

The detection of the degree of order by measuring the intensities of superlattice reflections is a common tool in transmission electron microscopy. However, deciding which type of order is present in the specimen, e.g., a homogeneous state of long-range order, fluctuations of the long-range ordered state on a mesoscopic scale or on a nanometer scale as may be expected under cascade producing irradiation, or short-range order, is a more difficult task. A detailed determination of the shape of the intensity peaks in the diffraction pattern and of the diffuse scattering contributions should be carried out.¹⁴ In the present work, this was not possible due to the small volume fraction of precipitates in the alloy. For the purpose of this investigation, we restrict ourselves to the discussion of the evolution of the intensity of the superlattice reflections and attribute the decrease from an initially complete long-range order into a lower ordered state in terms of the order parameter S . We show in the following that this assumption allows us to resolve the basic processes of disordering and dissolution operating under irradiation.

A. Disordering

The disordering rate of ordered phases depends on the type of irradiation and on the temperature, e.g., irradiation experiments with electrons with energy of typically 1 MeV show that an ordered phase will disorder, at sufficiently low temperature, after about 1 dpa,¹⁵⁻¹⁷ while ion and neutron irradiations induce disordering much more effectively: significant disorder is already created after 0.1 dpa.^{1,15,18}

An important question is obviously how large the degree of an average state of order S_∞ is, which can be obtained after very high fluences, i.e., for steady-state conditions. At very low temperatures the irradiation induces a totally disordered state. A residual degree of long-range order was observed below room temperature in many intermetallics [Ni_3Al , $NiAl$, $FeAl$ (Ref. 19)] under electron irradiation, whereas in the case of ion or neutron irradiation, complete disordering is generally reported. In particular, Nelson, Hudson, and Mazey¹ reported a completely disordered state of the γ' phase in the Nimonic PE16 alloy after irradiation at room temperature with 3-MeV nickel ions to a fluence of 0.1 dpa.

If the disordering process occurs randomly, then the time dependence of the order parameter is simply given by $S(t) = S_0 \exp(-\epsilon Kt)$ where ϵ is a parameter characterizing the effectiveness of the disordering process. Its magnitude depends on the type and temperature of irradiation. Experimentally, it is extracted from the initial disordering rate and has values of typically 1–3 dpa⁻¹ for electron irradiation^{15,17} and 10–100 dpa⁻¹ for ion or neutron irradiation.^{15,16} The parameter ϵ was estimated to be about 15 in the case of 3-MeV Ni^+ ion irradiation of the compound Ni_3Si at room temperature.²⁰ Hence a fluence of 1 dpa of heavy ion irradiation would reduce the order parameter by more than six orders of magnitude, according to the above exponential expression. This is in contrast to the present results, as in our experiment a residual intensity is observed up to fluences as high as 1 dpa. Although the present results seem to be at variance with earlier experiments,¹ they have been confirmed for the alloy Ni_3Al recently.²¹ Under the same irradiation conditions as used for the present investigation, nonvanishing intensities of superlattice reflections were observed at room temperature up to a fluence of 5 dpa, indeed indicating a residual degree of order $S_\infty > 0$.

A nonvanishing degree of order for high fluences can only be understood if a significant reordering occurs during irradiation. Several processes are proposed in the literature.¹⁵ The main locally operating reordering mechanism is the direct restoration during the production of the damage itself, i.e., annealing of a cascade, replacement sequence or uncorrelated recombination of vacancies and interstitials. In heavy ion irradiation the dominant process of atomic redistribution is connected with the production and annealing of defects (i.e., antisites, vacancies and interstitials) inside cascades,²² which can be described in the framework of a thermal-spike model.²³

In addition to the local reordering by cascades, there will be reordering by long-range migration of point defects. For this mechanism the reordering rate depends on

the product of the concentration and the jump frequency of the point defects.²⁴

Reordering by vacancy migration is well understood and discussed in many ordered systems under thermal conditions and under irradiation, for example in Cu_3Au (Ref. 25) or in Ni_4Mo .¹⁷ The contribution of vacancies to the reordering of the γ' phase at room temperature is assumed to be negligibly small, as the vacancies become mobile only above 400 K.^{26,27} The estimated migration energy is 1.35 to 1.38 eV in the Ni-Al system including Ni_3Al .

The effect of interstitial diffusion on the ordering kinetics needs a more detailed discussion. We have estimated the influence of interstitials on the reordering kinetics in the ion-irradiated $L1_2$ structure. The reordering rate was calculated using a simple rate equation approach for the evolution of the interstitial concentration as a function of irradiation time.²⁸ As no stationary state is established at room temperature at a fluence of 1 dpa, the radiation-induced order-disorder transformation had to be calculated with a time-dependent reordering rate. We used for the calculations the migration energies estimated by Dimitrov *et al.* from recovery curves in Ni-Al alloys, i.e., $E_m^i = 0.16\text{--}0.28$ eV for different Ni-Ni dumbbell interstitial configurations.^{26,27} Using a fractional production of freely migrating interstitials of 0.01 and $c_s = 10^{-5}$ for the defect sink concentration,^{13,29} a significant reordering by long-range interstitial migration would indeed be predicted, when assuming the interstitials to order as effectively as vacancies. This is, however, not likely to be the case for the following reasons: (i) according to molecular-dynamics calculations, the interstitials in Ni_3Al migrate mainly via Ni-Ni dumbbells on the Ni lattice, which do not contribute to reordering; (ii) no significant recovery stage was observed between 190 K and room temperature indicating that the reordering process is not likely to be caused by a long-range diffusion of interstitials;^{26,27} (iii) the experimental results of the evolution of the state of order in initially completely ordered Ni_3Al under electron irradiation below room temperature^{19,30} cannot be understood if it is presumed that the efficiency of interstitial ordering is similar to vacancy ordering. The data for Ni_3Al by Liu and co-workers^{19,30} show a completely disordered structure for temperatures $T < 190$ K, and an increasing steady-state value S_∞ for temperatures $T > 190$ K, which are well below the temperature of vacancy migration.²⁶ If the interstitials would contribute to reordering as vacancies, only a small reduction of the initially completely ordered structure is predicted for a fluence of 1 dpa and temperatures as low as 150 K. This is at variance to the experimental findings of Liu and co-workers.^{19,30}

We can therefore conclude that a long-range migration of point defects cannot account for the residual degree of order observed in this investigation after ion irradiation at room temperature.

A nonvanishing value S_∞ of the order parameter of an ordered phase after long irradiation times can be understood in the framework of a thermal-spike induced disordering.²³ Molecular-dynamics calculations have shown that this concept indeed can be applied to ordered al-

loys.^{22,31,33} The concept of disordering by cascades using the thermal spike is based on the idea of a localized deposition of high-energy density in the cascade region. In the volume of the cascade an effective temperature can be defined which determines the ordered state in that volume. It depends on the rate of energy dissipation in the cascade whether the disordered volume is quenched in.³² A quantitative application of this concept to the experimentally measured size of disordered zones in Ni_3Si as a function of matrix temperature has shown that significant reordering happens at room temperature.²³ A fit of the model to results obtained on Ni_3Si irradiated by 3-MeV Ni^+ ions at 350 K (Ref. 20) indicates that the maximum disordered volume shrinks during reordering by 20%. This would correspond to a nonvanishing order parameter of $S_\infty \simeq 0.2$ in that case. The time evolution of the mean order parameter of the γ' phase is then given by²³

$$S_{\gamma'}(t) = S_\infty + (S_0 - S_\infty) \exp(-\varepsilon K t), \quad (1)$$

where S_∞ depends on the temperature. S_∞ is small for low temperatures and increases for higher temperatures. The residual value of the intensity of the superlattice reflections observed between 0.1 and 1 dpa can be understood qualitatively in the framework of Eq. (1) with the parameters $\varepsilon = 15$ and $S_\infty = 0.2$. Work on the monophase Ni_3Al intermetallics is under progress to get a more quantitative information.²¹

B. Dissolution

In the case of a two-phase alloy, a cascade producing irradiation at low temperatures may cause the dissolution of a precipitated phase by atomic mixing. The dissolution of the γ' phase in the alloy Nimonic PE16 at room temperature has been studied by FIM-AP.³⁴⁻³⁷ It was shown that this process can be described by a diffusion-controlled transport process of the solute atoms into the surrounding matrix. The second Fick's equation

$$\frac{\partial c(r,t)}{\partial t} = D \nabla^2 c(r,t) \quad (2)$$

determines the temporal evolution of the radial concentration $c(r,t)$ where D is a constant diffusion coefficient and r is the spatial vector having its origin at the center of the spherical precipitate. With appropriate boundary conditions, the solution of Eq. (2) for increasing diffusion times is shown in Fig. 6. The radiation-induced diffusion coefficient normalized by the displacement rate $D/K = 0.75 \text{ nm}^2 \text{ dpa}^{-1}$ was estimated by a quantitative analysis.³⁵ This value agrees well with published data of mixing diffusion coefficients.³⁸ It is obvious from this picture that at the beginning of the dissolution, the concentration inside of the precipitate remains constant, while the concentration at its boundary falls quickly.

Reordering of a disordered volume by cascades is generally expected only if the local concentration inside of the precipitates allows the formation of the γ' phase. In order to estimate the precipitate volume in which reordering of a damaged volume is possible, we assume that the local concentration of Al and Ti must be larger than a

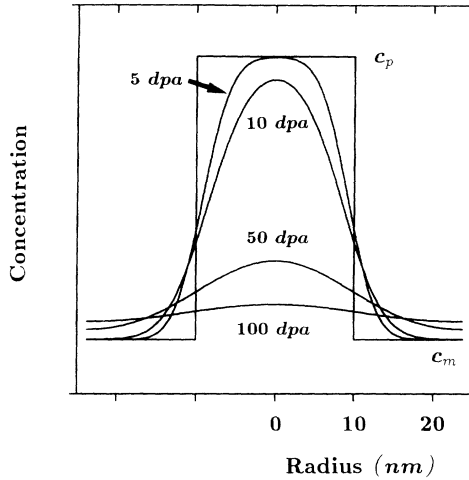


FIG. 6. Calculated diffusion profiles modeling the dissolution of the γ' precipitates under irradiation. The value of the diffusion coefficient normalized by the displacement rate is $0.75 \text{ nm}^2 \text{ dpa}^{-1}$. c_p and c_m are the precipitate and matrix concentration of the diffusing species, respectively.

given concentration c_{lim} . The limiting concentration of the γ' phase in the phase diagram of Ni_3Al may be taken as an approximation of c_{lim} . If during diffusion the local concentration of Al and Ti becomes smaller than c_{lim} , then reordering of the damaged volume is not possible. The critical radius $R_{\text{lim}}(t)$ of a precipitate in which the concentration is above c_{lim} , and which can therefore reorder, is then given by the implicit equation

$$c(R_{\text{lim}}(t), t) = c_{\text{lim}}. \quad (3)$$

The dependence of the critical radius R_{lim} on fluence is shown in Fig. 7 for an initial precipitate radius of 10 nm, a dissolution rate given by $D/K = 0.75 \text{ nm}^2 \text{ dpa}^{-1}$ and a limiting concentration $c_{\text{lim}} = 0.24$. The fast decrease of R_{lim} at smaller fluences corresponds physically to the fast reduction of the concentration gradient at the matrix/precipitate interface. As already pointed out, the concentration inside the precipitate remains practically constant at the beginning of the dissolution process.

Furthermore, the above discussed disordering process and the dissolution process have time constants which differ by about two orders of magnitude: whereas most of the disordering is completed after a fluence of 0.1 dpa, dissolution of precipitates with an initial diameter of 20 nm needs fluences of more than 5 dpa. Therefore, we may introduce an *effective* order parameter $S_{\text{eff}}(t)$ as the *product* of a dissolution term, which describes the remaining fraction of ordered γ' precipitate volume, and of the order parameter $S_{\gamma'}(t)$ inside the γ' phase [see Eq. (1)]:

$$S_{\text{eff}}(t) = \frac{N_v(t)}{N_v(0)} \frac{R_{\text{lim}}^3(t)}{R_0^3} S_{\gamma'}(t). \quad (4)$$

In Fig. 8, the order parameter $S_{\gamma'}$ and the effective order parameter S_{eff} are plotted as a function of the fluence

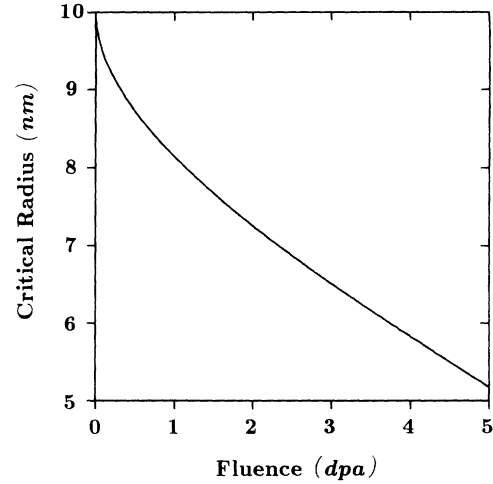


FIG. 7. Calculated critical radius above which the composition of the precipitates does not yet correspond to the composition of the γ' phase. The initial radius of the precipitates is 10 nm. The values were calculated assuming the dissolution mechanism displayed in Fig. 6 with a critical concentration $c_{\text{lim}}(\text{Al}+\text{Ti}) = 0.24$ and a dissolution rate of $D/K = 0.75 \text{ nm}^2 \text{ dpa}^{-1}$.

again for precipitates with an initial diameter of 20 nm, with the parameters $\epsilon = 15$, $S_{\infty} = 0.2$, and a dissolution rate $D/K = 0.75 \text{ nm}^2 \text{ dpa}^{-1}$. In this plot, we have taken into account that the precipitate number density N_v remains constant during irradiation.^{34,37} The curve $S_{\text{eff}}(t)$ reproduces in a qualitative way (i) the fast disordering of the γ' phase within 0.1–0.2 dpa, (ii) the plateau value of the intensities of the superlattice reflections observed between 0.1 and 1 dpa, and (iii) their final disappearing due to the dissolution of the precipitates.

The fact that, after a fluence of 2 dpa, the precipitates have disordered although they are still present in concen-

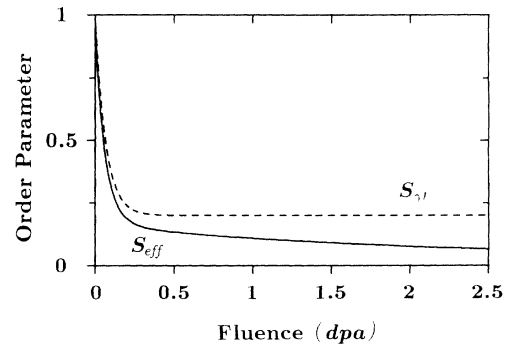


FIG. 8. The order parameter $S_{\gamma'}$ of a single γ' phase material and the effective order parameter S_{eff} of γ' precipitates taking into account the dissolution process are calculated as a function of the fluence according to Eqs. (1) and (4). The plotted curves were calculated assuming a dissolution rate $D/K = 0.75 \text{ nm}^2 \text{ dpa}^{-1}$, a limiting concentration $c_{\text{lim}}(\text{Al}+\text{Ti}) = 0.24$, a disordering parameter $\epsilon = 15$ and a stationary value of the order parameter $S_{\infty} = 0.2$.

tration, [see Fig. 4(b)] allows us to conclude that, for a heavy ion irradiation at room temperature, the γ' precipitates *first* disorder and *then* dissolve. This sequence of disordering dissolution is in general agreement with the results of detailed numerical investigations of the radiation-induced destabilization of the ordered B_2 and L_{12} structures by Martin and co-workers.³⁻⁶

The irradiation temperature influences the observed two-step process. The consequences of increasing the temperature are (i) a reduction of the disordering efficiency and (ii) an increase of long-range diffusion by a vacancy mechanism. We will discuss irradiation experiments at higher temperatures in a forthcoming paper.³⁹

V. CONCLUSION

We have reported in this paper results concerning the disordering and dissolution of γ' precipitates under cascade producing irradiation. The disordering of the γ' phase at room temperature was investigated by following the intensity of superlattice reflections on diffraction patterns as a function of irradiation fluence. A rapid decrease of their intensity within 0.1 dpa was observed. The main finding is the existence of weak but measurable intensities between 0.1 and 1 dpa. Above 1 dpa, no superlattice reflections were detected, while the precipitates

could be still imaged in bright field after 2 dpa.

The following conclusions can be drawn:

(i) under cascade producing irradiation, the initially ordered γ' phase does not disorder completely after irradiation to a fluence of 1 dpa at room temperature;

(ii) the vanishing of the superlattice reflections for a fluence of more than 2 dpa is caused by the dissolution of the γ' precipitates;

(iii) the introduced effective order parameter S_{eff} allows a consistent description of both the disordering and the dissolution process.

The above conclusions demonstrate that, at room temperature, the precipitates first disorder and then dissolve.

ACKNOWLEDGMENTS

We are grateful to Dr. G. Martin for many discussions and helpful comments during the course of this work. Thanks are due to Dr. N. Wanderka and Dr. P. Bellon for assistance in the examination of the specimens at the electron microscopes. We are indebted to Dr. V. Naundorf, Dr. D. Mukherji, and Dr. M. Sundararaman for reading of the manuscript and valuable comments and suggestions. This work was supported by the French-German exchange program Procope.

¹R. S. Nelson, J. A. Hudson, and D. J. Mazey, *J. Nucl. Mater.* **44**, 318 (1972).

²J. A. Hudson, *J. Br. Nucl. Energy Soc.* **14**(2), 127 (1975).

³E. Salomons, P. Bellon, F. Soisson, and G. Martin, *Phys. Rev. B* **45**, 4582 (1992).

⁴F. Soisson, P. Bellon, and G. Martin, *Phys. Rev. B* **46**, 11 332 (1992).

⁵G. Martin, F. Soisson, and P. Bellon, *J. Nucl. Mater.* **205**, 301 (1993).

⁶M. Przybylowicz, P. Bellon, and G. Martin (unpublished).

⁷H. P. Degischer, W. Hein, H. Strecker, and R. P. Wahi, *Z. Metallkde.* **78**, 237 (1987).

⁸M. F. Ashby and L. M. Brown, *Philos. Mag.* **8**, 1649 (1963).

⁹P. M. Kelly, A. Jostsons, R. G. Blake, and J. G. Napier, *Phys. Status Solidi A* **31**, 771 (1975).

¹⁰S. J. B. Reed, *Electron Microprobe Analysis* (Cambridge University Press, Cambridge, England, 1975).

¹¹F. Bourdeau, Ph.D. thesis, T. U. Berlin **D83**, 1992.

¹²J. P. Biersack and L. G. Haggmark, *Nucl. Instrum. Methods* **174**, 257 (1980).

¹³A. Müller, V. Naundorf, and M.-P. Macht, *J. Appl. Phys.* **64**, 3445 (1988).

¹⁴C. L. Corey, B. Z. Rosenblum, and G. M. Greene, *Acta Metall.* **21**, 837 (1973).

¹⁵E. M. Schulson, *J. Nucl. Mater.* **83**, 239 (1979).

¹⁶K. C. Russell, *Mater. Sci. Eng.* **28**, 229 (1984).

¹⁷S. Banerjee and K. Urban, *Phys. Status Solidi A* **81**, 145 (1984).

¹⁸D. I. Potter, in *Phase Transformations During Irradiation*, edited by F. V. Nolfi (Applied Science, London, 1983).

¹⁹H. C. Liu, C. Kinoshita, and T. E. Mitchell, in *Phase Stability During Irradiation*, edited by J. R. Holland, L. K. Mansur,

and D. I. Potter (The Metallurgical Society of AIME, Warrendale, PA, 1981), p. 343.

²⁰D. I. Potter, O. G. Hernandez, and S. Lamond, in *Phase Stability During Irradiation* (Ref. 19), p. 329.

²¹C. Abromeit, S. Müller, and N. Wanderka (unpublished).

²²F. Gao and D. J. Bacon, *Philos. Mag.* (to be published).

²³C. Abromeit and H. Wollenberger, *J. Nucl. Mater.* **191-194**, 1092 (1992).

²⁴A. C. Dienes, *J. Phys. Chem. Solids* **4**, 177 (1958).

²⁵R. H. Zee and P. Wilkes, *Philos. Mag.* **A 42**, 463 (1980).

²⁶C. Dimitrov, B. Sitaud, X. Zhang, O. Dimitrov, U. Dedek, and F. Dworschak, *J. Phys. Condens. Matter* **4**, 10 199 (1992).

²⁷C. Dimitrov, B. Sitaud, X. Zhang, O. Dimitrov, U. Dedek, and F. Dworschak, *J. Phys. Condens. Matter* **4**, 10 211 (1992).

²⁸C. Abromeit and R. Poerschke, *J. Nucl. Mater.* **82**, 298 (1979).

²⁹M.-P. Macht, A. Müller, V. Naundorf, and H. Wollenberger, *Phys. Status Solidi A* **104**, 287 (1987).

³⁰H. C. Liu and T. E. Mitchell, *Acta Metall.* **31**, 863 (1983).

³¹F. Gao and D. J. Bacon, *Philos. Mag.* **67**, 275 (1993).

³²T. J. Black, M. L. Jenkins, C. A. English, and M. A. Kirk, *Proc. R. Soc. London Ser. A* **409**, 177 (1977).

³³T. Diaz de la Rubia, A. Caro, and M. Spaczer, *Phys. Rev. B* **47**, 11 483 (1993).

³⁴E. Camus, *Fortschritt-Bericht-VDI 310* (VDI-Verlag, Düsseldorf, 1993), Series 5.

³⁵E. Camus and C. Abromeit, *J. Appl. Phys.* **75**, 2373 (1994).

³⁶E. Camus and C. Abromeit, *Z. Metallkde.* **85**, 378 (1994).

³⁷E. Camus, F. Bourdeau, and C. Abromeit (unpublished).

³⁸H. Wollenberger, *Nucl. Instrum. Methods, Phys. Res. Sect. B* **48**, 493 (1990).

³⁹F. Bourdeau, E. Camus, and C. Abromeit (unpublished).

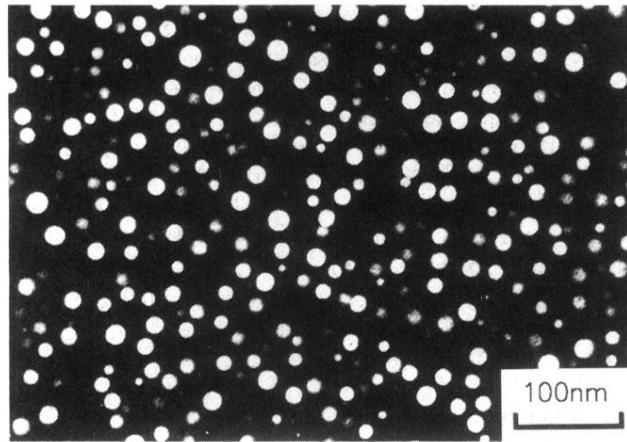


FIG. 1. Dark-field image of the γ' phase after solution annealing at 1313 K for 2 h and subsequent aging at 1025 K for 24 h. A $\{210\}$ superlattice reflection in the $\langle 211 \rangle$ reciprocal plane was used for imaging. The mean diameter of the precipitates and the volume fraction of the γ' phase are 19 ± 4 nm and 0.06 ± 0.02 , respectively.

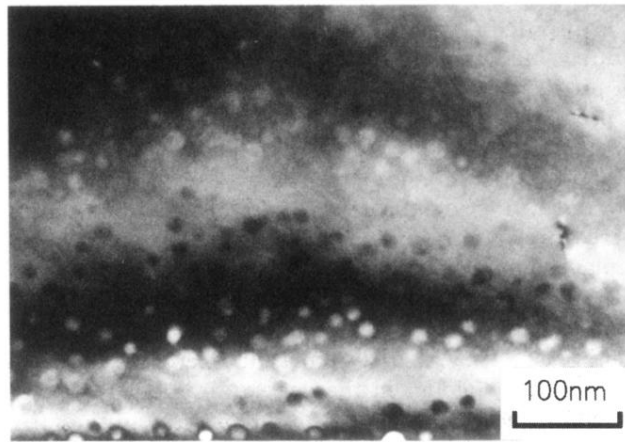


FIG. 2. Bright-field image of the γ' phase with a thickness contrast. The γ' precipitates have a larger extinction distance than the matrix and are imaged alternately in bright and dark contrast.

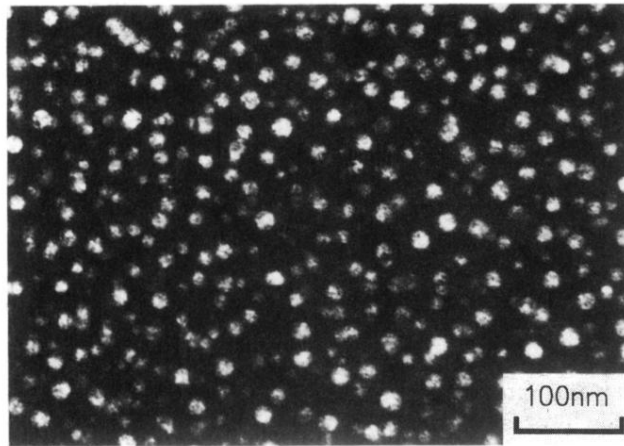


FIG. 3. Dark-field image of the γ' precipitates after irradiation with Ni self-ions at room temperature with a displacement rate of 10^{-3} dpa s^{-1} to a fluence of 0.05 dpa. A $\{210\}$ superlattice reflection in the $\langle 211 \rangle$ reciprocal plane was used for imaging.

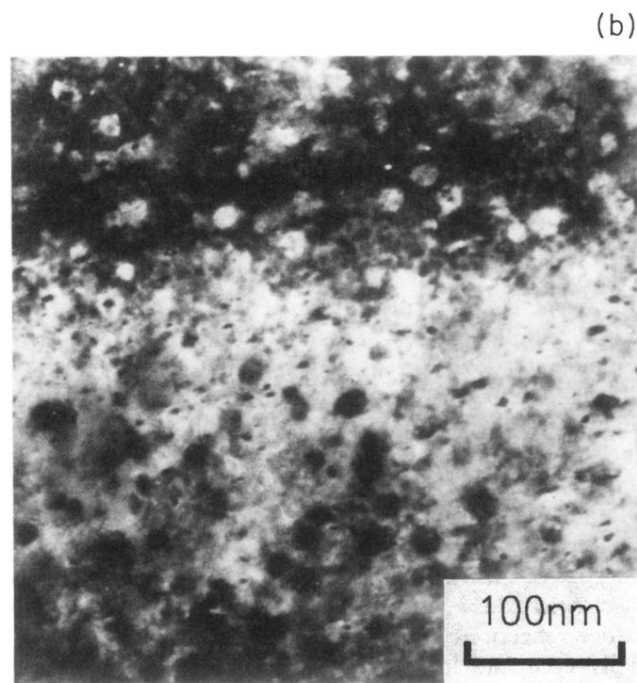
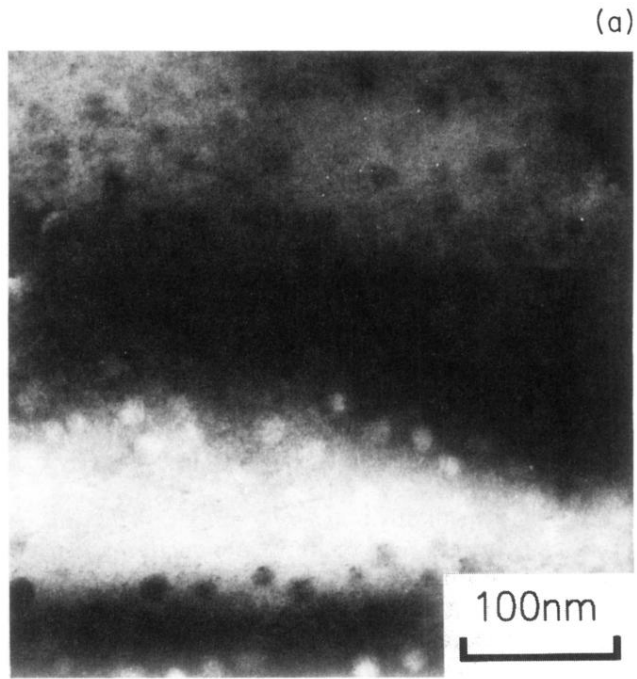


FIG. 4. Bright-field image of the γ' precipitates after irradiation with Ni self-ions at room temperature with a displacement rate of 10^{-3} dpa s^{-1} to fluences of (a) 1 dpa and (b) 2 dpa.

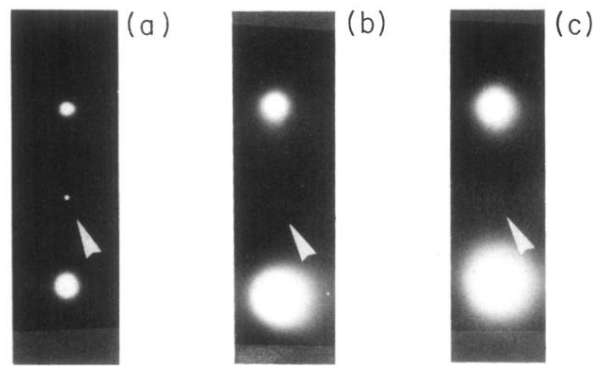


FIG. 5. Diffraction patterns of γ' containing specimens (a) before irradiation and after irradiation with Ni self-ions at room temperature with a displacement rate of 10^{-3} dpa s^{-1} to fluences of (b) 0.1 dpa and (c) 1 dpa.